



Contents lists available at ScienceDirect

Chinese Chemical Letters

journal homepage: www.elsevier.com/locate/cclet



Communication

2-Oxo-3,4-dihydropyrimido[4, 5-d] pyrimidines as new reversible inhibitors of EGFR C797S (Cys797 to Ser797) mutant

Xianglong Hu^{a,1}, Qiuju Xun^{a,1}, Tao Zhang^{b,1}, Su-Jie Zhu^{c,1}, Qian Li^a, Linjiang Tong^b, Mengzhen Lai^b, Tao Huang^a, Cai-Hong Yun^{d,*}, Hua Xie^{b,*}, Ke Ding^{a,*}, Xiaoyun Lu^{a,*}

^a International Cooperative Laboratory of Traditional Chinese Medicine Modernization and Innovative Drug Development of Chinese Ministry of Education (MOE), School of Pharmacy, Jinan University, Guangzhou 510632, China

^b Division of Antitumor Pharmacology, State Key Laboratory of Drug Research, Shanghai Institute of Materia Medica, Chinese Academy of Sciences, Shanghai 201203, China

^c Institute for Translational Medicine, College of Medicine, Qingdao University, Qingdao 266021, China

^d Department of Biochemistry and Biophysics, Institute of Systems Biomedicine, School of Basic Medical Sciences, Peking University Health Science Center, Beijing 100191, China

ARTICLE INFO

Article history:
Available online xxx

Keywords:
EGFR^{C797S} mutant
SARs
2-Oxo-3,4-dihydropyrimido[4,5-d]
pyrimidine
Clinical resistance
Fourth-generation inhibitors

ABSTRACT

Extensive structure–activity relationships (SARs) study of JND3229 was conducted to yield a series of new reversible 2-oxo-3,4-dihydropyrimido[4,5-d]pyrimidine privileged scaffold as EGFR^{C797S} inhibitors. One of the most potent compound **6i** potently suppressed EGFR^{L858R/T790M/C797S} kinase with an IC₅₀ value of 3.1 nmol/L, and inhibited the proliferation of BaF3 cells harboring EGFR^{L858R/T790M/C797S} and EGFR^{19D/T790M/C797S} mutants with IC₅₀ values of 290 nmol/L and 316 nmol/L, respectively. Further, **6i** dose-dependently induced suppression of the phosphorylation of EGFR^{L858R/T790M/C797S} and EGFR^{19D/T790M/C797S} in BaF3 cells. Compound **6i** may serve as a promising lead compound for further drug discovery overcoming the acquired resistance of non-small cell lung cancer (NSCLC) patients.

© 2019 Chinese Chemical Society and Institute of Materia Medica, Chinese Academy of Medical Sciences.
Published by Elsevier B.V. All rights reserved.

Epidermal growth factor receptor-tyrosine kinase inhibitors (EGFR-TKIs) have brought great benefits in the clinic for the treatment of non-small cell lung cancer (NSCLC) patients harboring EGFR-mutation. To date, three generations of EGFR inhibitors [1,2], e.g., gefitinib, erlotinib, afatinib, dacomitinib and osimertinib (AZD9291), have been approved by Food and Drug Administration (FDA). Particularly, the third generation EGFR Thr790 to Met790 mutant (T790M) inhibitor osimertinib, covalently binding to Cys797, demonstrated approximately 75% overall response rate (ORR) in EGFR^{T790M} mutation-positive NSCLC patients and was approved as the first-line treatment for metastatic NSCLC patients in 2018 [3–5]. However, EGFR tertiary Cys797 to Ser797 (C797S) point mutation arises rapidly after treatment of osimertinib in clinic, due to the fact that the less reactive serine797 fails to form a covalent bond with osimertinib [6,7]. EGFR^{C797S} mutation has become the most common acquired resistance to the third-generation EGFR-TKIs [8]. Thus,

it is highly urgent to develop the fourth-generation EGFR inhibitors to overcome EGFR^{C797S} mutation [9].

Several fourth-generation inhibitors of EGFR with different binding types have been reported [1,10], including the allosteric inhibitors EAI045 (**1a**) and JBJ-04-125-02 (**1b**) [11], and the ATP-competitive inhibitors **2–4** [12–15] (Fig. 1). Among them, the (2-hydroxy)phenyl-4-substituted quinazoline **2** and tri-substituted imidazole **3** displayed strong potency against EGFR^{C797S} kinase in biochemical assay, but neither cell-based activity nor *in vivo* efficacy of these molecules was disclosed. EAI045 (**1a**) and brigatinib (**4**) were both required to combine with EGFR antibody cetuximab or pantitumumab to demonstrate *in vivo* therapeutic efficacy [11,15]. Most recently, we have identified a pyrimidopyrimidinone-based derivative JND3229 (**5**) as a new reversible EGFR^{C797S} mutant inhibitor demonstrating both *in vitro* and *in vivo* mono-drug efficacy against the proliferation of EGFR^{C797S} mutated cancer cells [16]. Structure analysis indicated that JND3229 bound to the ATP binding site of EGFR^{C797S} with a reversible “U-shaped” configuration. The 2-oxo-3,4-dihydropyrimido[4,5-d]pyrimidine privileged core formed a bidentate hydrogen bond interactions with Met793, the 2-chlorophenyl group was directed toward the hydrophobic back pocket, and the carbonyl in pyrido[4,5-d]pyrimidine formed a hydrogen bond with Lys745 mediated by a

* Corresponding authors.

E-mail addresses: yunch@hsc.pku.edu.cn (C.-H. Yun), hxie@siml.ac.cn (H. Xie), dingke@jnu.edu.cn (K. Ding), luxy2016@jnu.edu.cn (X. Lu).

¹ These authors contributed equally to this work.

<https://doi.org/10.1016/j.cclet.2019.09.044>

1001-8417/© 2019 Chinese Chemical Society and Institute of Materia Medica, Chinese Academy of Medical Sciences. Published by Elsevier B.V. All rights reserved.

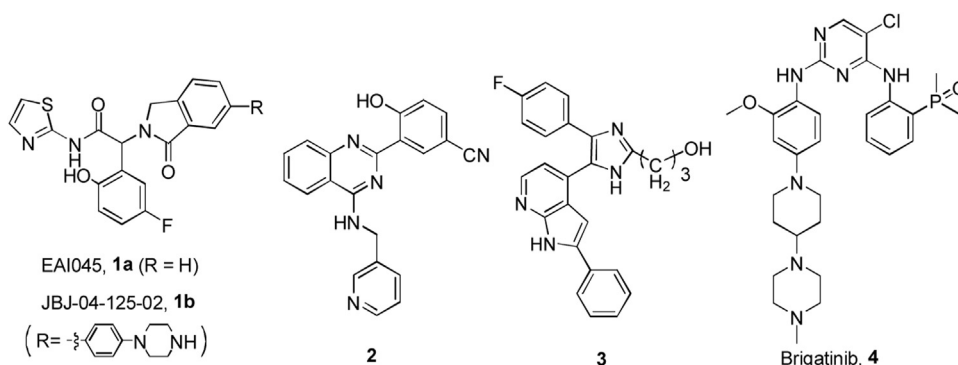


Fig. 1. The reported fourth generation EGFR inhibitors overcoming EGFR^{C797S} mutation.

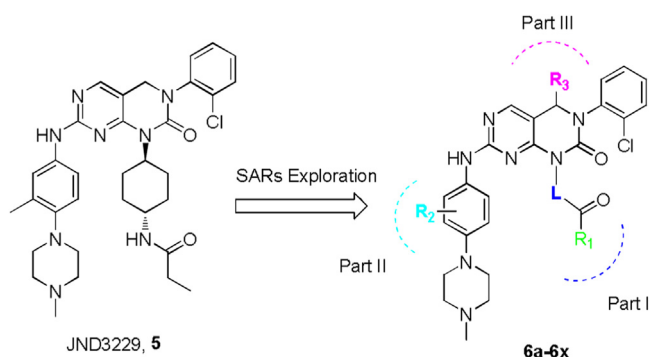


Fig. 2. The designed 2-oxo-3,4-dihydropyrimido[4,5-d] pyrimidines privileged scaffold based on JND3229.

water molecule. Herein, we would like to describe extensive structure-activity relationships (SARs) of this 2-oxo-3,4-dihydropyrimido[4,5-d]pyrimidine privileged scaffold based compounds (Fig. 2).

The synthetic routes of the designed 2-oxo-3,4-dihydropyrimido[4,5-d]pyrimidinyl analogues were outlined in Scheme 1. Briefly, reduction of 4-chloro-2-(methylthio)-pyrimidine-5-carboxylate (**7**) with diisobutyl aluminium hydride (DIBAL) gave (4-chloro-2-(methyl thio)pyrimidin-5-yl)methanol, which were subsequently oxidized by MnO_2 to yield aldehyde **9**. For compounds **6a–6u** and **6x**, **9** then reacted with BOC-protected aliphatic amines, followed by Borch reductive amination, cyclization and oxidation to yield key pyrimidopyrimidinone **14**. For compounds **6v** and **6w**, **9** went through Grignard reaction to give alcohol **15**, which followed by chlorination, nucleophilic substitution, cyclization and oxidation to yield key pyrimidopyrimidinone **20**. The intermediates **14** and **20** were respectively subjected to nucleophilic, deprotection and acylation reaction to give the title compounds **6a–6w**.

The kinase inhibitory activities of the title compounds were evaluated by the enzyme-linked-immunosorbent assay (ELISA) assay (Table 1). Osimertinib, staurosporine and JND3229 were used as positive controls to validate the screening conditions. As shown in Table 1, osimertinib potentially inhibits EGFR^{L858R/T790M}, while is less potent against EGFR^{L858R/T790M/C797S}. However, staurosporine, a broad spectrum of multi-kinase inhibitor, suppresses the enzymatic activity of the EGFR^{L858R/T790M} and EGFR^{L858R/T790M/C797S} mutants with low nanomolar IC_{50} values.

We firstly investigated the SARs on the linker L (Fig. 2) and the results were summarized in Table 1. Change of *trans*-cyclohexanamine in JND3229 with a *cis*-cyclopyrrolidinamine (**6a**) and linear ethylamine (**6b**) led to 14-fold and complete potency loss against

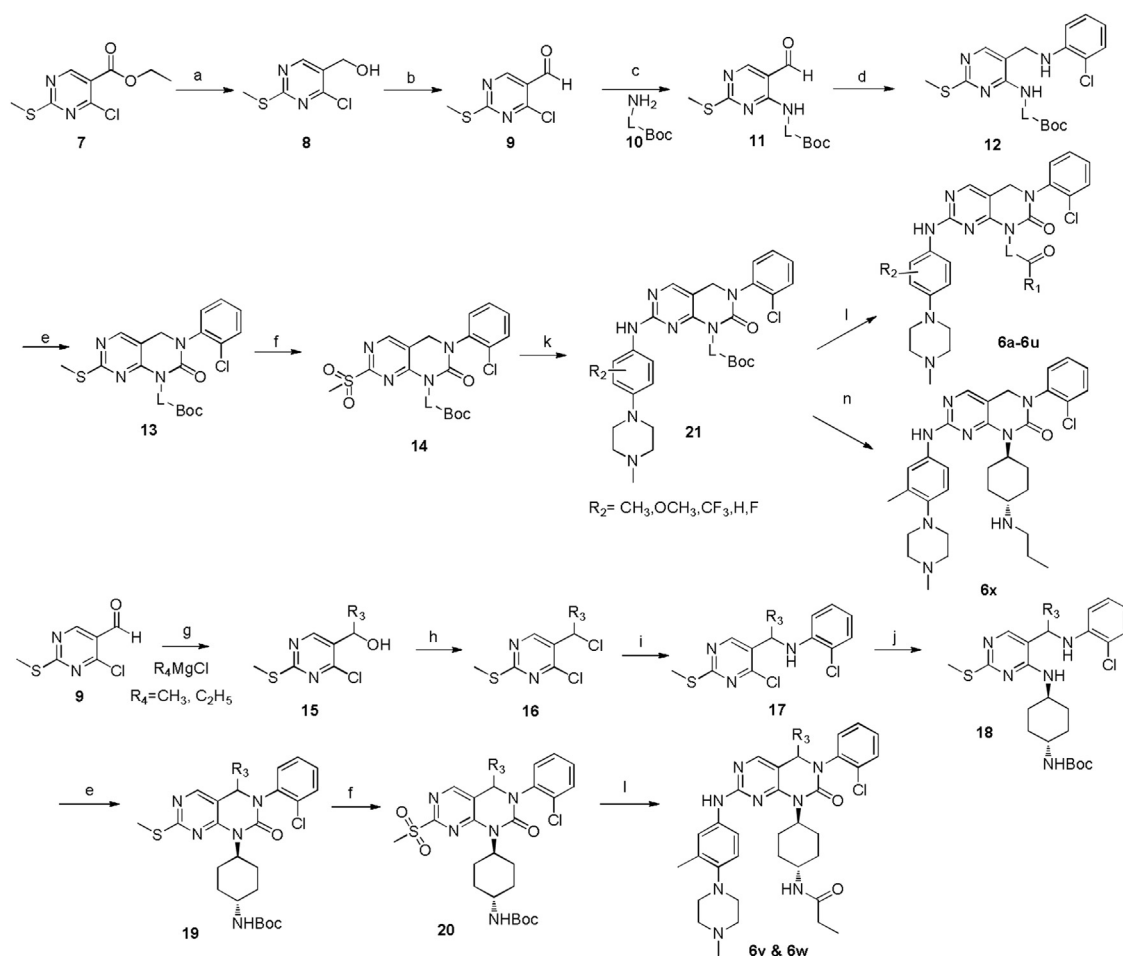
EGFR^{L858R/T790M/C797S}. When exocyclic N atom in the linker was incorporated into the cycloalkyl group, the resulting compounds (**6c–6h**) showed greatly decreased potency on EGFR^{L858R/T790M/C797S}. Compound **6i** with *cis*-cyclohexanamine instead of the *trans*-cyclohexanamine exhibited an IC_{50} value of 3.1 nmol/L against EGFR^{L858R/T790M/C797S}, which is comparable to that of JND3229. Moreover, this compound is 7-fold more potent than JND3229 with the inhibitory activity of EGFR^{L858R/T790M} double mutant. These results indicated that the cyclohexanamine group in the linker fraction was preferable for the high inhibitory activity.

After determined that the cyclohexanamine was the optimal substituent for the L part, we then turned to optimize the R1 substitution (Table 1). It was revealed that the ethyl in JND3229 could be replaced with a variety of relative small substituents (e.g., methyl (**6j**), isopropyl (**6k**), *tert*-butyl (**6l**)), without obviously affecting the EGFR inhibitory potency. However, when the ethyl was replaced with larger hydrophobic groups, including cyclopentyl (**6m**), or cyclohexyl (**6n**), and phenyl (**6o**), the resulting molecules displayed about 3- to 7-folds potency loss. For instance, **6o** with the phenyl substituent exhibited an IC_{50} value of 14.4 nmol/L against EGFR^{L858R/T790M/C797S}. Interestingly, introducing an N atom into this phenyl group in **6o** further reduced the compound's activity (**6p**, IC_{50} = 35.2 nmol/L). It was worthy to note that when the propionyl moiety in JND3229 was replaced with a propyl group, the resulting compound (**6x**) dramatically decreased the kinase inhibitory potency with an IC_{50} value of 139.7 nmol/L against EGFR^{L858R/T790M/C797S}. The investigation suggested that a critical interaction might exist between the carbonyl group and the protein.

The X-ray structure analysis of EGFR^{T790M/C797S} and JND3229 complex revealed that the methyl substituted phenylpiperazine moiety of JND3229 was exposed to a solvent accessible surface [16]. We then explored the preliminary SARs of 3'-methyl substituent. When the 3'-methyl group in JND3229 was replaced with 3'- CF_3 (**6r**) or changed to 2'-position (**6u**), the resulting compounds exhibited comparable activities, while replacement of 3'-methyl group with the other substituents, e.g., 3'-F (**6r**), 3'- OCH_3 (**6s**), or removal of it (**6t**), yielded compounds with potency loss ranging from 2- to 3-folds.

At last, we investigated the potential steric impact of R₃ position by substitution with methyl (**6v**) and ethyl (**6w**). The compound **6v** exhibited the equal activity compared to the parental compound JND3229, while the ethyl substituted compound **6w** displayed about 4-folds potency loss, suggesting that the bulky moieties were not tolerated at this site.

In order to get insight into the binding mode of *cis*-cyclohexanamine with EGFR^{T790M/C797S}, a co-crystal structure of **6i** complexed with EGFR^{T790M/C797S} was determined (Fig. 3A and Table S1 in Supporting information). It was indicated that **6i** bound



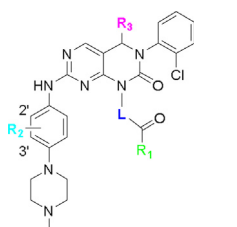
Scheme 1. General procedures for synthesis of compounds **6a–6u**, **6x**, **6v** and **6w**. Reagents and conditions: (a) DIBAL, THF, -78°C , 3–4 h, 88%; (b) MnO_2 , DCM, r.t., overnight, 86%; (c) CH_3CN , r.t., overnight, 70%–82%. (d) i) 2-chloroaniline, AcOH, PhCH_3 , 110°C , 110 $^{\circ}\text{C}$; ii) NaBH_4 , THF, 70°C , 50%–60%; (e) Triphosgene, DIPEA, DCM, 0°C , 70%–80%; (f) m-CPBA, DCM, r.t., 70%–80%; (g) R_3MgCl , THF, -40°C , 80%–90%; (h) DIPEA, POCl_3 , 0°C , 2 h, 70%–80%; (i) 2-chloroaniline, Acetonitrile, r.t., overnight, 80%–85%; (j) **10**, CH_3CN , r.t., overnight, 80%–90%; (k) 3-methyl-4-(4-methylpiperazin-1-yl)aniline, TFA, 2-butyl alcohol, 110°C , overnight, 40%–50%; (l) i) TFA, DCM, r.t.; ii) propionic acid, HATU, DIPEA, DCM, overnight, 30%–50%. (n) i) TFA, DCM, r.t.; ii) iodine propane, EtOH, DCM, 80°C , 20 h, 28%–35%.

to EGFR^{T790M/C797S} with a reversible “U-shaped” configuration with the “hinge” residue Met793. The 2-chlorophenyl group was directed toward the hydrophobic back pocket composed by Lys745, Glu762, Leu788, Met766 and Met790. Different conformations of cyclohexylamine caused the different binding patterns to protein. The carbonyl of amide in **6i** formed a hydrogen bond with Ser720 mediated by a water molecule, while the NH of amide in JND3229 formed a hydrogen bond with Leu718 mediated by another water molecule.

The antiproliferative activities of compounds **6a–6x** were also investigated against H1975 (EGFR^{L858R/T790M}) and BaF3 cells stably transfected with EGFR^{L858R/T790M/C797S} and EGFR^{19D/T790M/C797S} mutants (Table 1). It was showed that **6a–6x** exhibited moderate antiproliferative activities against H1975 and BaF3 cells harboring EGFR^{L858R/T790M/C797S} and EGFR^{19D/T790M/C797S} mutants, with IC_{50} values of 0.12–3.27 $\mu\text{mol/L}$, 0.29–>10 $\mu\text{mol/L}$ and 0.31–>10 $\mu\text{mol/L}$, respectively. Compound **6i** displayed the most potent antiproliferative activities against BaF3-EGFR^{L858R/T790M/C797S} and BaF3-EGFR^{19D/T790M/C797S} with IC_{50} values of 0.29 $\mu\text{mol/L}$ and 0.31 $\mu\text{mol/L}$, respectively, which is corresponding to that of biochemical kinase assay.

Further, the kinase inhibition of the most potent compounds **6i** and **6s** (both showed sub-micromolar activities against BaF3-EGFR^{L858R/T790M/C797S} and BaF3-EGFR^{19D/T790M/C797S}) was further validated by investigating its suppressive functions on the activation of EGFR in BaF3-EGFR^{L858R/T790M/C797S} and BaF3-EGFR^{19D/T790M/C797S} mutants. As shown in Fig. 4, compounds **6i** and **6s** caused a dose-dependent suppression of the phosphorylation of EGFR^{L858R/T790M/C797S} and EGFR^{19D/T790M/C797S} starting from the concentration of 100 nmol/L.

In summary, an extensive SAR investigation was conducted based on our recently disclosed 2-oxo-3,4-dihydropyrimido[4,5-d] pyrimidine privileged scaffold-based EGFR^{C797S} inhibitor JND3229. One of the most potent compound **6i** potentially suppressed EGFR^{L858R/T790M/C797S} kinase and inhibited the proliferation of BaF3 cells harboring EGFR^{L858R/T790M/C797S} and EGFR^{19D/T790M/C797S} mutants with IC_{50} values of 3.1 nmol/L, 290 nmol/L and 316 nmol/L, respectively. Compound **6i** dose-dependently induced suppression of the phosphorylation of EGFR^{L858R/T790M/C797S} and EGFR^{19D/T790M/C797S} in BaF3 cells starting from the concentration of 100 nmol/L. Compound **6i** may serve as a new generation of EGFR inhibitors for anticancer drug discovery.

Table 1
In vitro EGFR inhibition and anti-proliferation data of compounds **6a–6j**.


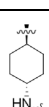

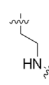
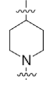
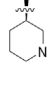
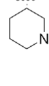
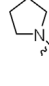
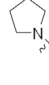
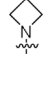
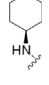
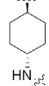
Cpds	L	R ₁	R ₂	R ₃	Kinase IC ₅₀ (nmol/L)		Cellar IC ₅₀ (μmol/L)		
					EGFR ^{L858R/DM}	EGFR ^{L858R/TM1}	TM1H1975	BaF3-EGFR ^{L858R/TM1}	BaF3-EGFR ^{19D/TM2}
JND3229		C ₂ H ₅	3'-CH ₃	H	30.5 ± 3.3	5.8 ± 2.5	0.31 ± 0.01	0.51 ± 0.08	0.32 ± 0.11
6a		C ₂ H ₅	3'-CH ₃	H	248.1 ± 90.4	45.1 ± 32.3	0.61 ± 0.08	1.29 ± 0.04	1.82 ± 0.67
6b		C ₂ H ₅	3'-CH ₃	H	>1000	>1000	1.76 ± 0.33	>10	>10
6c		C ₂ H ₅	3'-CH ₃	H	103.2 ± 20.6	66.7 ± 27.9	0.38 ± 0.12	1.41 ± 0.19	1.66 ± 0.49
6d		C ₂ H ₅	3'-CH ₃	H	>1000	>1000	1.59 ± 0.52	9.04 ± 0.85	9.64 ± 0.03
6e		C ₂ H ₅	3'-CH ₃	H	511.5 ± 103.9	>1000	2.00 ± 0.15	8.80 ± 0.75	7.10 ± 2.14
6f		C ₂ H ₅	3'-CH ₃	H	869.4 ± 117.5	>1000	1.43 ± 0.53	7.90 ± 1.51	9.44 ± 0.21
6g		C ₂ H ₅	3'-CH ₃	H	711.0 ± 153.7	>1000	1.89 ± 0.59	9.45 ± 0.31	4.35 ± 1.89
6h		C ₂ H ₅	3'-CH ₃	H	232.6 ± 5.7	596.0 ± 344.5	3.27 ± 0.94	>10	>10
6i		C ₂ H ₅	3'-CH ₃	H	5.1 ± 3.0	3.1 ± 0.9	0.12 ± 0.09	0.29 ± 0.17	0.31 ± 0.12
6j		CH ₃	3'-CH ₃	H	5.1 ± 0.8	4.2 ± 1.2	0.68 ± 0.07	1.55 ± 0.24	1.32 ± 0.49

Table 1 (Continued)

Cpds	L	R ₁	R ₂	R ₃	Kinase IC ₅₀ (nmol/L)		Cellar IC ₅₀ (μmol/L)		
					EGFR ^{L858R/DM}	EGFR ^{L858R/TM1}	TM1H1975	BaF3-EGFR ^{L858R/TM1}	BaF3-EGFR ^{19D/TM2}
6k			3'-CH ₃	H	19.1 ± 2.0	6.7 ± 2.0	0.51 ± 0.09	1.09 ± 0.47	1.75 ± 0.08
6l			3'-CH ₃	H	27.6 ± 7.0	7.9 ± 1.6	0.65 ± 0.04	1.36 ± 0.53	2.11 ± 0.14
6m			3'-CH ₃	H	38.0 ± 9.8	15.8 ± 2.9	0.84 ± 0.15	1.43 ± 0.42	2.04 ± 0.28
6n			3'-CH ₃	H	65.8 ± 12.0	43.1 ± 9.3	1.11 ± 0.13	0.99 ± 0.01	1.03 ± 0.004
6o			3'-CH ₃	H	17.4 ± 3.3	14.4 ± 2.5	1.55 ± 0.31	1.75 ± 0.24	1.92 ± 0.14
6p			3'-CH ₃	H	29.2 ± 4.2	35.2 ± 5.8	2.38 ± 0.78	2.37 ± 0.36	2.74 ± 0.34
6q		C ₂ H ₅	3'-F	H	19.9 ± 5.4	11.0 ± 1.9	0.31 ± 0.13	0.66 ± 0.06	1.28 ± 0.50
6r		C ₂ H ₅	3'-CF ₃	H	4.0 ± 2.5	8.8 ± 6.0	1.80 ± 0.25	1.20 ± 0.48	0.89 ± 0.49
6s		C ₂ H ₅	3'-OCH ₃	H	25.7 ± 9.2	13.2 ± 3.2	0.38 ± 0.16	0.47 ± 0.15	0.52 ± 0.18
6t		C ₂ H ₅	3'-H	H	24.4 ± 12.0	18.3 ± 3.3	0.55 ± 0.17	0.58 ± 0.28	1.13 ± 0.44
6u		C ₂ H ₅	2'-CH ₃	H	5.8 ± 2.2	9.1 ± 2.6	1.76 ± 0.30	0.58 ± 0.28	1.13 ± 0.84

Table 1 (Continued)

Cpds	L	R ₁	R ₂	R ₃	Kinase IC ₅₀ (nmol/L)		Cellar IC ₅₀ (μmol/L)		
					EGFR ^{L858R/DM}	EGFR ^{L858R/TM1}	TM1H1975	BaF3-EGFR ^{L858R/TM1}	BaF3-EGFR ^{19D/TM2}
6v		C ₂ H ₅	3'-CH ₃	CH ₃	39.8 ± 19.0	6.2 ± 1.7	1.48 ± 0.55	2.46 ± 0.61	7.20 ± 4.46
6w		C ₂ H ₅	3'-CH ₃	C ₂ H ₅	23.3 ± 4.2	22.8 ± 2.4	3.15 ± 0.91	2.29 ± 0.36	9.67 ± 0.11
6x					196.9 ± 71.9	139.7 ± 35.1	2.24 ± 0.20	1.49 ± 0.65	2.47 ± 0.64
AZD9291	–				2.5 ± 0.7	297.7 ± 125.6	<0.016	3.39 ± 0.42	9.27 ± 0.37
Staurosporine	–				26.7 ± 4.7	4.6 ± 3.0	0.03 ± 0.01	0.01 ± 0.01	0.05 ± 0.01

Note: DM: L858R/T790M, TM1: L858R/T790M/C797S, TM2: 19D/T790M/C797S.

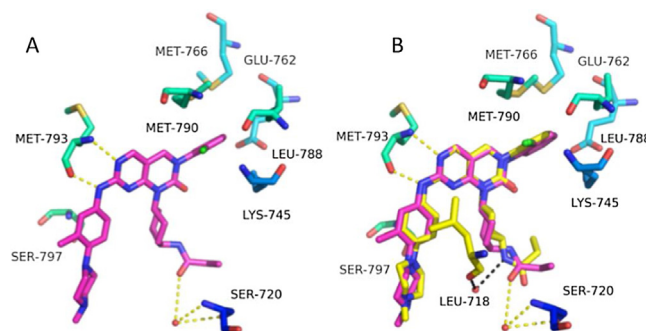


Fig. 3. (A) The X-ray crystal structure of **6i** with EGFR^{T790M/C797S} (PDB ID: 6JRX). (B) Overlay the **6i** and JND3229 in EGFR^{T790M/C797S} (PDB ID: 5ZTO). The EGFR kinase is shown in green and blue stick and ribbon representation. **6i** and JND3229 are shown in purple and yellow stick. Hydrogen bonds are indicated by yellow and black hatched lines to key amino acids. Water is represented as red dots.

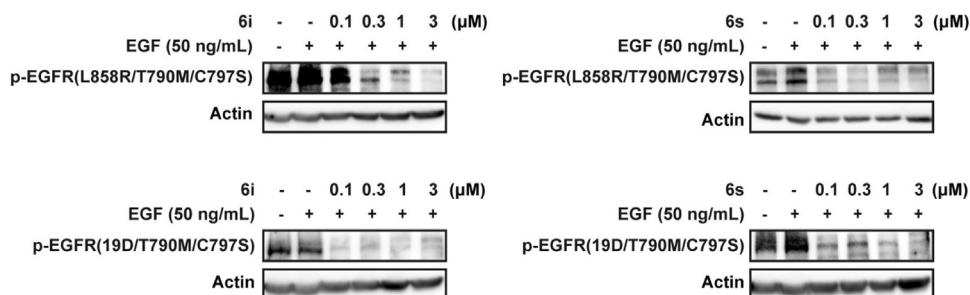


Fig. 4. Compounds **6i** and **6s** potentially suppressed the phosphorylation of EGFR^{L858R/T790M/C797S} and EGFR^{19D/T790M/C797S} in BaF3 cells. Cells were treated with or without compounds **6i** and **6s** for 4 h at indicated concentration, respectively. Cells were then stimulated by 50 ng/ml EGF for 10 min and harvested for western blot analysis.

Declaration of competing interest

The authors declare that they have no known competing financial interests or personal relationships that could have appeared to influence the work reported in this paper.

Acknowledgments

The authors appreciate the financial support from National Natural Science Foundation of China (Nos. 81922062, 81874285 and 81673285), Guangdong International Science and Technology

Cooperation Project (No. 2018A050506043), Guangzhou City Key Laboratory of Precision Chemical Drug Development (No. 201805010007) and Institutes for Drug Discovery and Development of Chinese Academy of Science (No. CASIMM0120185006).

Appendix A. Supplementary data

Supplementary material related to this article can be found, in the online version, at doi:<https://doi.org/10.1016/j.ccllet.2019.09.044>.

References

- [1] X. Lu, L. Yu, Z. Zhang, et al., *Med. Res. Rev.* 38 (2018) 1550–1581.
- [2] Z. Song, Y. Ge, C. Wang, et al., *J. Med. Chem.* 59 (2016) 6580–6594.
- [3] D.A. Cross, S.E. Ashton, S. Ghiorghiu, et al., *Cancer Discov.* 4 (2014) 1046–1061.
- [4] S.L. Greig, *Drugs* 76 (2016) 263–273.
- [5] J.C. Soria, Y. Ohe, J. Vansteenkiste, et al., *N. Engl. J. Med.* 378 (2018) 113–125.
- [6] Z. Piotrowska, M.J. Niederst, C.A. Karlovich, *Cancer Discov.* 5 (2015) 713–722.
- [7] K.S. Thress, C.P. Paweletz, E. Felip, et al., *Nat. Med.* 21 (2015) 560–562.
- [8] M.J. Niederst, H. Hu, H.E. Mulvey, et al., *Clin. Cancer Res.* 21 (2015) 3924–3933.
- [9] T. Grabe, J. Lategahn, D. Rauh, et al., *ACS Med. Chem. Lett.* 9 (2018) 779–782.
- [10] L. Chen, W. Fu, L. Zheng, et al., *J. Med. Chem.* 61 (2018) 4290–4300.
- [11] (a) Y. Jia, C.H. Yun, E. Park, et al., *Nature* 534 (2016) 129–132;
(b) C. To, J. Jang, T. Chen, et al., *Cancer Discov.* 9 (2019) 926–943.
- [12] H. Park, H.Y. Jung, S. Mah, S. Hong, *Angew Chem. Int. Ed. Eng.* 56 (2017) 7634–7638.
- [13] M. Gunther, M. Juchum, G. Kelter, et al., *Angew Chem. Int. Ed. Eng.* 55 (2016) 10890–10894.
- [14] M. Juchum, M. Gunther, E. Doring, et al., *J. Med. Chem.* 60 (2017) 4636–4656.
- [15] K. Uchibori, N. Inase, M. Araki, *Nat. Commun.* 8 (2017) 14768.
- [16] X. Lu, T. Zhang, S. Zhu, *ACS Med. Chem. Lett.* 9 (2018) 1123–1127.